RYDBERG STATES IN LASER FIELDS

G. Alber and P. Zoller

Institute for Theoretical Physics
University of Innsbruck, A-6020 Innsbruck, Austria

1. INTRODUCTION

Rydberg states play an important role as intermediate or final states in laser induced processes studied in atoms and molecules. A typical one photon excitation process of Rydberg states $|\epsilon_n\rangle$ from a low-lying atomic state $|g\rangle$ is characterized by three parameters: The spectral width of the laser pulse $\Delta\omega_L \approx \hbar/T_P$ whose pulse duration is T_P, the Rabi frequencies Ω_n associated with the transitions $|g\rangle \longrightarrow |\epsilon_n\rangle$ and the level spacing between adjacent Rydberg states $\Delta\omega_n \approx 2Ry/\hbar(-\epsilon_n/Ry)^{3/2}$. Depending on the relative magnitudes of these parameters we can distinguish between three dynamical cases: (1) The simplest situation arises, if we excite an isolated Rydberg state well below threshold ($\Delta\omega_n > \Omega_n, \Delta\omega_L$). This regime is well understood on the basis of a two-(or few-) level approximation, which treats the coupling between the resonant atomic states nonperturbatively and takes into account the influence of all other nonresonant states perturbatively. On the contrary, cases (2) and (3), which correspond to excitation by a short ($\Delta\omega_L > \Delta\omega_n, \Omega_n$) or intense ($\Omega_n > \Delta\omega_n, \Delta\omega_L$) laser pulse and arise if we are exciting sufficiently close to a Rydberg threshold, are not so well understood. In the extreme situation of excitation directly at a Rydberg threshold both (infinitely) many Rydberg states and part of the adjoining electron continuum are excited and traditional theoretical approaches based on a few-level approximation[1] for the bound-bound transitions $|g\rangle \longrightarrow |\epsilon_n\rangle$ or the pole-approximation[1] as far as the bound-free transitions $|g\rangle \longrightarrow |\epsilon\rangle$ are concerned break down.

Recently we have developed a theory[2], which is capable of describing laser excitation close to a Rydberg threshold. It is based on the observation that the photon absorption process $|g\rangle \longrightarrow |\epsilon_n\rangle$ takes place in a region around the atomic nucleus (≡ reaction zone), which is small in comparison with the extent of highly excited Rydberg states. This *finite range* of the radiative coupling allows us to use concepts of quantum defect theory (QDT)[3] and to derive closed analytical expressions for transition amplitudes, whose time dependence can conveniently be studied with the help of a *multiple scattering expansion*. This expansion expresses these amplitudes as an infinite sum over contributions due to all

A. D. Bandrauk (ed.), *Atomic and Molecular Processes with Short Intense Laser Pulses*

classical paths of the excited Rydberg electron (Kepler orbits). In particular, for excitation close to a Rydberg threshold, i.e. cases (2) and (3), it leads directly to the physical picture of a (radial) Rydberg wave packet, which is generated inside the reaction zone and moves in the Coulomb potential of the ionic core.

The main purpose of this paper is to discuss laser excitation close to a Rydberg threshold. Therefore in section two we study generation and detection of Rydberg wave packets by short laser pulses and in section three we deal with the excitation of a Rydberg series by an intense laser pulse (generalized Rabi problem).

2. SHORT LASER PULSES

According to our introductory remarks a short laser pulse implies $\Delta\omega_L > \Omega_n$ so that the initial atomic state $|g\rangle$ is undepleted and the excitation of the Rydberg electron can be determined by time dependent perturbation theory in the laser field. For times t long after the interaction with the laser pulse the state of the atom is therefore approximately given by $|\Psi(t)\rangle = e^{-i\epsilon_g t}|g\rangle + |\Psi_g(t)\rangle$ with the state of the excited Rydberg electron described by

$$|\Psi_g(t)\rangle = i\int_{-\infty}^{+\infty} dt'\; e^{-iH_A(t-t')}\,\vec{d}\cdot\vec{\epsilon}\;\mathcal{E}(t')\;e^{-i\bar{\epsilon}t'}\;|g\rangle\;. \qquad (2.1)$$

H_A is the atomic Hamiltonian, $\vec{d}$ the dipole operator, $\vec{\epsilon}$ and $\mathcal{E}(t)$ the polarization and slowly varying electric field amplitude of the laser field and $\bar{\epsilon} = \epsilon_g + \omega$ is the mean excited energy (We use Hartree atomic units). From Equ.(2.1) we immediately notice that the laser excitation process affects only a spatial region of the size of $|g\rangle$. This region (≡ reaction zone) is small in comparison with the extent of the highly excited Rydberg states so that the laser excitation process is *localized in space*.

A short laser pulse also implies $\Delta\omega_L > \Delta\omega_n$ so that many Rydberg states are excited. In the time domain this condition states that the interaction time between atom and laser field T_P is small in comparison with the mean classical orbit time $T_{\bar{\epsilon}} = 2\pi(-2\bar{\epsilon})^{-3/2}$ of the excited electron in the Coulomb potential of the ionic core. The laser excitation process is therefore also *localized in time*. Both conditions, namely localization of the photon absorption process in space and time imply that a (radial) Rydberg wave packet is generated[4,5]. Note that due to dipole selection rules only a few angular momentum eigenstates are excited so that only the radial coordinate of the Rydberg electron is localized.

The center of this wave packet performs a periodic motion in the Coulomb potential of the ionic core with period $T_{\bar{\epsilon}}$. If we are exciting a multi-electron atom with one valence electron, for example, the electrostatic potential due to the ionic core deviates from a pure $1/\rho$-Coulomb form inside the core region, which is essentially identical with the small reaction zone where the initial laser excitation process has taken place. Therefore, whenever the excited wave packet returns to the reaction zone it experiences an additional electron-ion scattering due to this modified core potential, which can be characterized by a

scattering matrix element $\chi = e^{i2\pi\alpha}$. Due to the fact that inside the reaction zone there is no difference between energy normalized Rydberg- and continuum states close to the Rydberg threshold (ϵ=0) χ is a slowly varying function of energy across threshold. Above threshold (ϵ>0) $\pi\alpha$ is a continuum phase shift and below (ϵ< 0) α is the quantum defect of the excited Rydberg series. This physical picture suggests that $|\Psi_g(t)\rangle$ can be represented by a multiple scattering expansion as a sum over contributions due to all these subsequent (below threshold) electron-ion scattering events, which take place inside the reaction zone and are characterized by a scattering matrix χ (compare with Equ.(3.6)).

The periodic motion of the generated wave packet can be probed by any process which is also localized in space and time. One example is a two-photon Raman process with two time delayed short laser pulses. In such a process a radial electronic wave packet is generated by a first short laser pulse, which excites an atom from an initial state $|g\rangle$. A second short laser pulse then deexcites this wave packet after a time delay $\Delta t >> T_P$ by inducing a transition to some low-lying bound state $|f\rangle$. As excitation and deexcitation (≡ stimulated recombination) both take place inside a small reaction zone around the atomic nucleus we expect a large Raman transition probability whenever $\Delta t \approx mT_{\overline{\epsilon}}$. This can be seen in Fig.1 where the Raman transition probability is plotted in arbitrary units as a function of $\Delta t/T_{\overline{\epsilon}}$ in the case of excitation of a single Rydberg series. Each peak at $\Delta t \approx mT_{\overline{\epsilon}}$ is associated with a stimulated recombination of the electron-ion complex. The broadening of the recombination peaks reflects the spreading of the generated wave packet. After sufficiently long times (here $\Delta t \gtrsim 5T_{\overline{\epsilon}}$) the wave packet has spread out over the whole extent of its orbit so that contributions due to subsequent returns to the reaction zone overlap in time thus giving rise to a complicated interference pattern.

Additional interesting effects can arise in multi-electron atoms. Figs.2 show the Raman transition probability in the case of excitation of two Rydberg series, which are coupled by configuration interaction (coupling parameter r=0.02) and converge to different ionization thresholds ($\epsilon_1 = 4.7 \cdot 10^{-5}$, ϵ_2=0 a.u.). The first short laser pulse now generates a Rydberg wave packet in each channel with mean classical orbit times T_1 and T_2 (here $2T_2 \approx 3T_1$). In this case we expect a large Raman transition probability whenever $\Delta t \approx m_1T_1 + m_2T_2$. Recombination peaks associated with values $m_1 > 0$ and $m_2 > 0$ are possible, because with each return to the inner turning point of its orbit the wave packet can be scattered into the other channel by an inelastic (below threshold) electron-ion collision inside the reaction zone, which can be characterized by an off-diagonal matrix element of the approximately energy independent scattering matrix χ. The transition amplitude associated with a particular recombination peak (m_1,m_2) in Figs.2 is proportional to excitation- and deexcitation dipole matrix elements multiplied with scattering matrix elements of χ. So the amplitude of the peak (1,1), for example, is proportional to $(\mathcal{D}^{(-)}_{2f}\chi_{21}\mathcal{D}^{(-)}_{1g} + \mathcal{D}^{(-)}_{1f}\chi_{12}\mathcal{D}^{(-)}_{2g})$ and its value therefore strongly depends on the relative phases of the various photoionization dipole matrix elements $\mathcal{D}^{(-)}_{ig}$, $\mathcal{D}^{(-)}_{if}$ i=1,2. This is apparent from Figs. 2a and 2b. Whereas in Fig.2a $\mathcal{D}^{(-)}_{1g}/\mathcal{D}^{(-)}_{2g} = \mathcal{D}^{(-)}_{1f}/\mathcal{D}^{(-)}_{2f} = 1$ in Fig.2b $\mathcal{D}^{(-)}_{1g}/\mathcal{D}^{(-)}_{2g} = -\mathcal{D}^{(-)}_{1f}/\mathcal{D}^{(-)}_{2f} = 1$ and the peak (1,1) has dissapeared due to destructive interferences between the

two contributing quantum paths. Eventually both generated wave packets overlap (here at $\Delta t \approx 2T_2 \approx 3T_1$) and interfere quantum mechanically. Whether this interference is constructive (Fig.2b) or destructive (Fig.2a) also strongly depends on the relative phases of the photoionization dipole matrix elements.

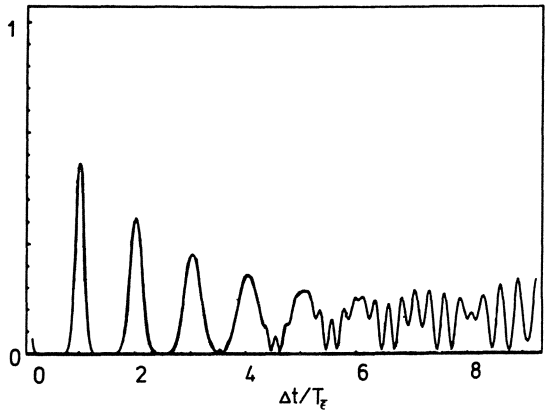

Fig.1: Raman transition probability as a function of time delay $\Delta t/T_{\overline{\epsilon}}$ with T_P=10ps, $T_{\overline{\epsilon}}$ =94ps.

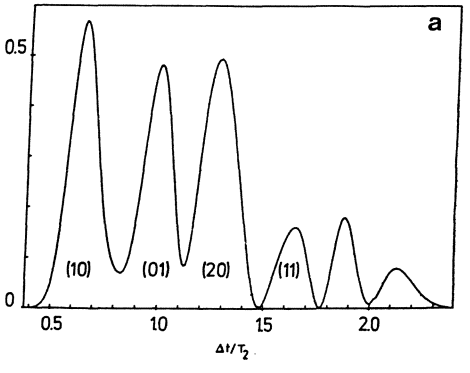

Fig.2a: Raman transition probability as a function of $\Delta t/T_2$ with $T_{P_1}=T_{P_2}$=14ps, $T_2=1.5\cdot T_1$=107ps, $\mathcal{D}_{1g}^{(-)}/\mathcal{D}_{2g}^{(-)} = \mathcal{D}_{1f}^{(-)}/\mathcal{D}_{2f}^{(-)} = 1$.

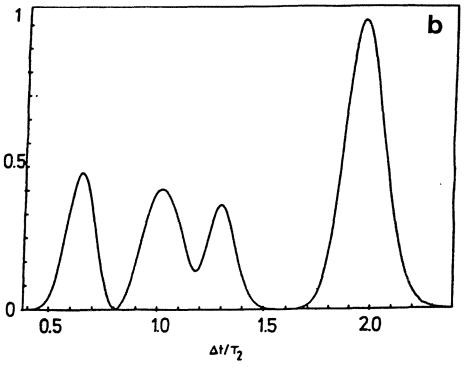

Fig.2b: Same as Fig.2a but with $\mathcal{D}_{1g}^{(-)}/\mathcal{D}_{2g}^{(-)} = -\mathcal{D}_{1f}^{(-)}/\mathcal{D}_{2f}^{(-)} = 1$.

3. INTENSE LASER PULSES

We consider excitation of a Rydberg series with quantum defect α from a low-lying atomic state $|g\rangle$ by an intense laser pulse, which is turned on instantaneously at t=0 and whose electric field envelope $\mathcal{E}(t)$ is constant for t>0. In particular we are interested in situations where the initial state $|g\rangle$ is depleted and many Rydberg states (and possibly part of the adjoining electron continuum) are excited so that the traditional two-(or few-) level approximation is not applicable. The state of the atom at time t is approximately given by $|\Psi(t)\rangle = |g\rangle a_g(t) + |F(t)\rangle$ with $|F(t)\rangle$ characterizing the time evolution of the excited electron. Taking the Laplace transform of $|\Psi(t)\rangle$ and neglecting ionization from the excited Rydberg states to higher electron continua we find in the dipole- and rotating wave approximation the system of equations

$$(z - \epsilon_g) a_g(z) + \langle g | \vec{d}\cdot\vec{\epsilon}^{\,*} \mathcal{E}^* | F(z+\omega)\rangle = i \qquad (3.1)$$

$$(z + \omega - H_A)\ |F(z+\omega)\rangle + \vec{d}\cdot\vec{\epsilon}\,\mathcal{E}\,|g\rangle\ a_g(z) = 0$$

with $|\Psi(t)\rangle = 1/2\pi \int_{-\infty+i0}^{+\infty+i0} dz\ e^{-izt}\ |\Psi(z)\rangle$. In the language of QDT these equations describe the coupling between a bound channel $|g\rangle$ and a free channel $|F(z+\omega)\rangle$[3]. According to Equs.(3.1) the Laplace transform $a_g(z)$ is given by

$$a_g(z) = i\ [\ z - \epsilon_g - \Sigma\ (z+\omega)\ ]^{-1} \qquad (3.2a)$$

with the resonant part of the self energy

$$\Sigma\ (\epsilon) = \langle\ g\ |\vec{d}\cdot\vec{\epsilon}^{\,*}\ \mathcal{E}^*\ \frac{1}{\epsilon - H_A + i0}\ \vec{d}\cdot\vec{\epsilon}\ \mathcal{E}|\ g\ \rangle = \qquad (3.2b)$$

$$= \begin{cases} \delta\omega - i\gamma/2 & (\epsilon > 0) \\ \delta\omega + \gamma/2\ \cot\pi(\nu+\alpha) & (\epsilon = -1/2\nu^{-2} < 0)\ . \end{cases}$$

(The final result for $\Sigma(\epsilon)$ can be obtained with the help of QDT methods or the Poisson summation formula)[2]. $\delta\omega$ is a contribution to the quadratic Stark shift of the initial state $|g\rangle$ and $\gamma = 2\pi\ |\langle\epsilon|\vec{d}\cdot\vec{\epsilon}\ \mathcal{E}|g\rangle|^2$ is the ionization rate according to Fermi's Golden rule and characterizes the radiative coupling between $|g\rangle$ and the excited channel. It is important to note that both parameters are approximately energy independent across the Rydberg threshold (ϵ=0), because inside the reaction zone, where the laser excitation process $|g\rangle \longrightarrow |\epsilon_n\rangle$ takes place and which is of the size of the initial state $|g\rangle$, there is no difference between energy normalized Rydberg- and continuum states close to threshold. This reflects the *localization* of the laser excitation process *in space*.

In order to determine the time evolution of $a_g(t)$ we have to invert the Laplace transform. Traditionally this is done with the help of contour integration in the complex z-plane. This approach leads to a *dressed state representation*, which expresses $a_g(t)$ as a sum over contributions due to all dressed states and a cut contribution from the electron continuum(ϵ>0)[2]. The dressed state energies $\tilde{\epsilon}_n = z_n + \omega = -1/2\tilde{\nu}_n^{-2} < 0$ are

associated with the poles of $a_g(z)$ at z_n. From Equs.(3.2) we find in our case the implicit transcendental equation $\tilde{\epsilon}_n = -1/2\ (n - \alpha - \mu(\tilde{\epsilon}_n))^{-2}$ for the dressed states so that the influence of the radiative coupling is characterized by the intensity dependent quantum defect

$$\mu(\epsilon) = -1/\pi\ \arctan(\gamma/2\ (\epsilon - \bar{\epsilon})^{-1}) \qquad (3.3)$$

with $\bar{\epsilon} = \epsilon_g + \omega + \delta\omega = -1/2\bar{\nu}^{-2}$. The appearance of this quantum defect is not surprising, because it is well known that mixing of an isolated bound state into an electron continuum leads to an additional continuum phase shift $\pi\mu(\epsilon)$. In laser excitation such a phase shift gives rise to laser-induced autoionizing-like resonances whereas in the process of laser-assisted electron-ion scattering, which is described by the scattering matrix

$$\tilde{\chi}(\epsilon) = e^{2i\pi(\alpha+\mu(\epsilon))}, \qquad (3.4)$$

it manifests itself in a "capture-escape" resonance[6]. Furthermore, continuum phase shifts correspond to quantum defects in the bound state region[3]. So we finally find in the *dressed state representation*[2]

$$a_g(t) = \sum_n e^{-i(\tilde{\epsilon}_n-\omega)t} 1/\pi\ \tilde{\nu}_n^{-3} \frac{\gamma/2}{(\tilde{\epsilon}_n-\bar{\epsilon})^2 + (\gamma/2)^2(1+2/\pi\gamma\cdot\tilde{\nu}_n^{-3})} + \qquad (3.5)$$

$$i/2\pi\ e^{-i(\bar{\epsilon}-\omega)t}\left\{e^{-\gamma t/2}[E_1(-i\bar{\epsilon}t-\gamma t/2)-2i\pi ST(\bar{\epsilon})] - e^{\gamma t/2}E_1(-i\bar{\epsilon}t+\gamma t/2)\right\}$$

with the exponential integral $E_1(x)$ and the unit step function ST(x). In the limit $\gamma << \bar{\nu}^{-3}$ we are exciting an isolated Rydberg state well below threshold and Equ.(3.5) reduces to the two-level result.

In the case of an intense laser pulse, however, $\gamma > \bar{\nu}^{-3}$ and many dressed states contribute to Equ.(3.5). In this limit it is more convenient to expand $a_g(z)$ in terms of the rapidly oscillating function $e^{i2\pi\nu}$ (Note that $2\pi\nu$ is just the classical action along a closed Kepler orbit of energy ϵ). This way we obtain the *multiple scattering expansion*[2]

$$a_g(t) = e^{-i(\bar{\epsilon}-\omega)t}\ e^{-\gamma t/2} + \qquad (3.6)$$

$$\sum_{m=1}^{\infty} \int_{-\infty}^{0} d\epsilon e^{-i(\epsilon-\omega)t}[i(\epsilon-\bar{\epsilon}+i\gamma/2)^{-1}\mathcal{D}_{\epsilon g}^{(-)}]e^{2i\pi\nu}[\tilde{\chi}(\epsilon)e^{2i\pi\nu}]^{m-1}$$

$$[\mathcal{D}_{\epsilon g}^{(-)} i(\epsilon-\bar{\epsilon}+i\gamma/2)^{-1}]$$

with the complex photoionization dipole matrix elements $\mathcal{D}_{\epsilon g}^{(-)} = -i\ e^{i\pi\alpha} \langle\epsilon|\vec{d}\cdot\vec{\epsilon}|g\rangle$. If $\gamma >> \bar{\nu}^{-3}$ we can evaluate the various energy integrals in equ.(3.6) in the stationary phase approximation and the dominant contributions arise from energies $\epsilon_s(m,t)$, which fullfill the stationary phase condition $t = T_{\epsilon_s}(m,t)$.

In the case of laser excitation close to the photoionization threshold by an intense pulse the physical interpretation of Equ.(3.6) is straight forward. For times $t<<T_{\bar{\epsilon}}$ the stationary phase contributions to Equ.(3.6) are negligible and the initial state probability is exponentially decaying with a rate γ. The laser excitation process is therefore not only *localized* in space but also *in time*, because the characteristic interaction time $1/\gamma$ ($\equiv$ depletion time of $|g\rangle$) is short in comparison with the mean classical orbit time $T_{\bar{\epsilon}}$. This implies that a radial electronic wave packet is generated. The exponential decay reflects the fact that at times $t<<T_{\bar{\epsilon}}$ this wave packet has not yet "felt" the outer turning point of its Kepler orbit and therefore behaves like in a true ionization process above threshold. For times $t\gtrsim T_{\bar{\epsilon}}$ the stationary phase contributions associated with $m=1,2,...$ become important. They describe the periodic motion of the excited wave packet in the Coulomb potential of the ionic core. In particular, the m-th term is the contribution due to the m-th return of this wave packet to the reaction zone, where it can be deexcited back to the initial state $|g\rangle$. The periodic recombinations of the electron-ion complex inside the reaction zone manifest themselves in pulsations of $|a_g(t)|^2$ with period $T_{\bar{\epsilon}}$. Equ.(3.6) shows that the m-th recombination peak centered at $t\approx mT_{\bar{\epsilon}}$ does not only contain information about the initial excitation- and final deexcitation process but also about the $(m-1)$ intermediate laser-assisted electron-ion scattering events inside the reaction zone, which are characterized by $\tilde{\chi}(\epsilon)$ of Equ.(3.4).

Figs.3 show the initial state probability $|a_g(t)|^2$ as a function of $t/T_{\bar{\epsilon}}$ for $\gamma=10^{-6}$a.u. and different values of $\bar{\epsilon}$. In Fig.3a $1/\gamma>T_{\bar{\epsilon}}$ and we observe the typical Rabi oscillations, which are slightly perturbed due to the presence of the nonresonant Rydberg states. In Figs.3b and 3c the laser excitation process is localized in time, i.e. $1/\gamma<T_{\bar{\epsilon}}$, and we see the characteristic exponential decay for $t<<T_{\bar{\epsilon}}$ and the pulsations with period $T_{\bar{\epsilon}}$ for $t\gtrsim T_{\bar{\epsilon}}$. As soon as the generated Rydberg wave packet has spread out over the whole extent of its orbit contributions due to successive returns to the reaction zone overlap in time and give rise to a complicated interference pattern. In Fig.3c we are exciting so close to threshold that this already happens at $t\gtrsim T_{\bar{\epsilon}}$.

Until now we have neglected photon absorption from Rydberg states to higher electron continua. Due to the large extent of highly excited Rydberg states it is not obvious that these transitions are also of finite range and it is therefore not clear how to include them into our treatment. However, it has recently been shown by Giusti-Suzor and Zoller[7] that the range of the radiative coupling ρ_R as far as Rydberg-free or free-free transitions are concerned is determined by the frequency ω and the intensity I of the laser pulse and is roughly given by $\rho_R\approx \max\{\omega^{-2/3}, \sqrt{I}\cdot\omega^{-2}\}$ (The a.u. of laser intensity is $I_0=1.4\cdot10^{17}$W/cm^2). This implies that for optical frequencies and not too high laser intensities photon absorption is of finite range even as far as these kind of transitions are concerned. This is an important result, because it allows us to include ionization from the excited Rydberg states in a straight forward manner into our approach and, more generally, to treat *configuration interaction* and *laser coupling* in a *unified way* due to the fact that both take place inside a reaction zone, which is small in

comparison with the extent of highly excited Rydberg states. All the physical processes inside this reaction zone can therefore be characterized by a laser-assisted electron-ion scattering matrix $\tilde{\chi}(\epsilon)$, which is a slowly varying function of energy across a Rydberg threshold as inside the reaction zone there is no difference between energy normalized Rydberg- and continuum states close to threshold. With the help of this general scattering matrix it is straight forward to derive multiple scattering expansions for the time evolution of various transition amplitudes and to study the threshold behaviour (compare with Equ.(3.6)).

Fig.3d shows $|a_g(t)|^2$ in the case of an additional decay channel of the Rydberg states (here due to autoionization with channel coupling parameter $\gamma=10^{-2}$ and q=20). Whereas in Fig.3c the time averaged "mean" initial state probability (dashed curves in Figs.3c and 3d) reaches a non zero stationary value in the long time limit reflecting population trapping in $|g\rangle$ the additional decay channel in Fig.3d finally leads to complete depletion of the initial state.

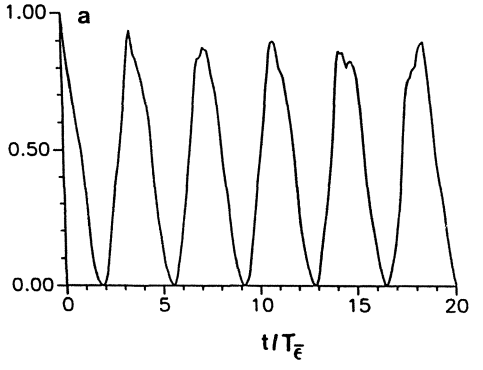

Fig.3a: Initial state probability as a function of $t/T_{\bar{\epsilon}}$ for $\gamma=10^{-6}$a.u. and $\bar{\epsilon}= -2\cdot10^{-4}$a.u.

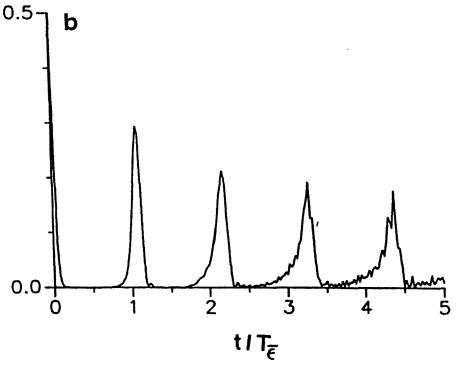

Fig.3b: Same as Fig.3a but with $\bar{\epsilon}= -1.25\cdot10^{-5}$a.u.

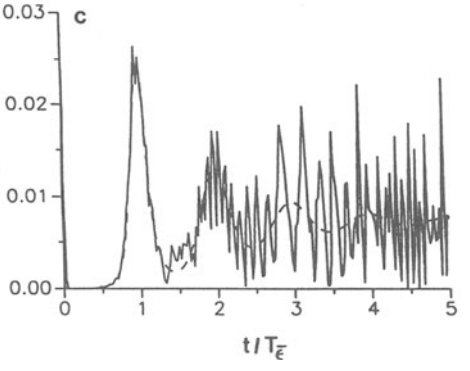

Fig.3c: Same as Fig.3a but with $\bar{\epsilon}= -4\cdot10^{-6}$a.u.

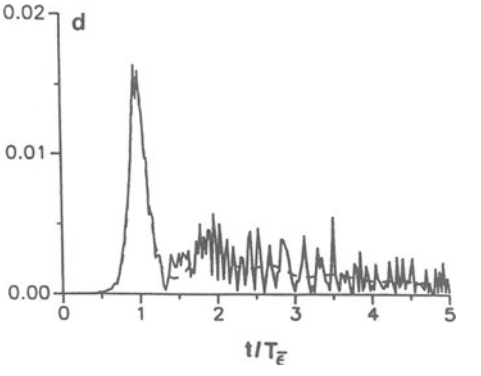

Fig.3d: Same as Fig.3c but with an additional decay channel.

ACKNOWLEDGMENT

This work was supported by the Austrian "Fonds zur Förderung der wissenschaftlichen Forschung" under contract number P6008P.

REFERENCES

1. C.Cohen-Tannoudji, B.Diu and F.Laloe, "Qantum Mechanics" (Wiley, 1977)
2. G.Alber and P.Zoller, Phys.Rev.A (submitted)
3. M.J.Seaton, Rep.Prog.Phys **46**, 167(1983)
4. G.Alber, H.Ritsch and P.Zoller, Phys. Rev. A**34**,1058(1986)
5. W.A.Henle,H.Ritsch and P.Zoller, Phys.Rev.A (in print)
6. L.Dimou and F.H.M.Faisal in "Photons and Continuum States of Atoms and Molecules" edited by N.K.Rahman, C.Guidotti and M.Allegrini (Springer, 1986)
7. A.Giusti-Suzor and P.Zoller, Phys.Rev.A (submitted)